

Fast robust correlation for high dimensional data

Jakob Raymaekers and Peter J. Rousseeuw*

Department of Mathematics, KU Leuven, Belgium

February 4, 2018

Abstract

The product moment covariance is a cornerstone of multivariate data analysis, from which one can derive correlations, principal components, Mahalanobis distances and many other results. Unfortunately the product moment covariance and the corresponding Pearson correlation are very susceptible to outliers (anomalies) in the data. Several robust measures of covariance have been developed, but few are suitable for the ultrahigh dimensional data that are becoming more prevalent nowadays. For that one needs methods whose computation scales well with the dimension, are guaranteed to yield a positive semidefinite covariance matrix, and are sufficiently robust to outliers as well as sufficiently accurate in the statistical sense of low variability. We construct such methods using data transformations. The resulting approach is simple, fast and widely applicable. We study its robustness by deriving influence functions and breakdown values, and computing the mean squared error on contaminated data. Using these results we select a method that performs well overall. It is illustrated on genomic data with 12,000 variables and color video data with 920,000 dimensions.

Keywords: anomaly detection, covariance matrix, data transformation, fast computation, outliers.

*This research has been supported by projects of Internal Funds KU Leuven.

1 Introduction

The most widely used measure of correlation is the product-moment correlation coefficient. Its definition is quite simple. Consider a paired sample, that is $\{(x_1, y_1), \dots, (x_n, y_n)\}$ where the two variables are the column vectors $X_n = (x_1, \dots, x_n)^T$ and Y_n . Then the *product moment* of X_n and Y_n is just the inner product

$$\text{PM}(X_n, Y_n) = \frac{1}{n} \langle X_n, Y_n \rangle = \frac{1}{n} X_n^T Y_n = \text{ave}_{i=1}^n x_i y_i . \quad (1)$$

When the (x_i, y_i) are i.i.d. observations of a stochastic vector (X, Y) the population version is the expectation $E[XY]$. The product moment (1) lies at the basis of many concepts. The *empirical covariance* of X_n and Y_n is the ‘centered’ product moment

$$\text{Cov}(X_n, Y_n) = \frac{n}{n-1} \text{PM}(X_n - \text{ave}(X_n), Y_n - \text{ave}(Y_n)) \quad (2)$$

with population version $E[(X - E[X])^T(Y - E[Y])]$. Therefore (1) can be seen as a ‘covariance about zero’. And finally, the product-moment correlation is given by

$$\text{Cor}(X_n, Y_n) = \frac{n}{n-1} \text{PM}(z(X_n), z(Y_n)) \quad (3)$$

where the z-scores are defined as $z(X_n) = (X_n - \text{ave}(X_n))/\text{Stdev}(X_n)$ with the standard deviation $\text{Stdev}(X_n) = \sqrt{\text{Var}(X_n)} = \sqrt{\text{Cov}(X_n, X_n)}$.

The product-moment quantities (1)–(3) satisfy $\text{PM}(X_n, Y_n) = \text{PM}(Y_n, X_n)$ and $\text{PM}(X_n, X_n) \geq 0$. They have several nice properties. The **independence property** states that whenever X and Y are independent we have $\text{Cov}(X, Y) = 0$ (assuming the expectations exist). Secondly, when our data set $\mathbf{X}_{n,d}$ has n rows (cases) and d columns (variables, dimensions) we can assemble all the product moments between the variables in a $d \times d$ matrix

$$\text{PM}(\mathbf{X}_{n,d}) = \frac{1}{n} \mathbf{X}_{n,d}^T \mathbf{X}_{n,d} . \quad (4)$$

The **PSD property** says that the matrix (4) is positive semidefinite, which is crucial. For instance, we can carry out a spectral decomposition of the covariance (or correlation) matrix, which forms the basis of principal component analysis. When $d < n$ the covariance matrix will typically be positive definite hence invertible, which is essential for many multivariate methods such as the Mahalanobis distance and discriminant analysis. The third

property is **speed**: due to their simple definitions the product moment, covariance and correlation matrices can be computed very fast, even in high dimensions d .

Despite these attractive properties, it has been known for a long time that the product-moment covariance and correlation are overly sensitive to outliers in the data. For instance, even adding a single far outlier can change the correlation from 0.9 to zero or to -0.9 .

Many robust alternatives to the Pearson correlation have been proposed in order to reduce the effect of outliers. The first one was probably Spearman's (1904) correlation coefficient, in which the x_i and y_i are replaced by their ranks. Also the quadrant correlation (Mosteller, 1946) is based on ranks. Such methods do not measure a linear relation but rather a monotone one, which may or may not be preferable in a given application. Many authors have used rank correlations for high dimensional problems. For instance, Liu et al. (2012) and Öllerer and Croux (2015) used them to estimate sparse high-dimensional precision matrices yielding graphical models.

A second approach is based on the identity

$$\text{Cor}(X, Y) = \frac{\text{Var}(z(X) + z(Y)) - \text{Var}(z(X) - z(Y))}{\text{Var}(z(X) + z(Y)) + \text{Var}(z(X) - z(Y))} \quad (5)$$

in which Gnanadesikan and Kettenring (1972) proposed to replace the nonrobust variance by a robust scale estimator. This approach is quite popular, see e.g. (Ma and Genton, 2001; Maronna and Zamar, 2002; Shevlyakov and Oja, 2016). It does not satisfy the independence property however, and the resulting correlation matrix is not PSD so it needs to be modified.

Thirdly, one can start by computing a robust multivariate covariance matrix \mathbf{C} such as the Minimum Covariance Determinant (MCD) method of Rousseeuw (1984). Then we can define a robust correlation measure between variables X_j and X_k by

$$R(X_j, X_k) := C_{jk} / \sqrt{C_{jj}C_{kk}} \quad (6)$$

In this way we do produce a PSD matrix, but we lose the independence property. In fact, the robust correlation between two variables depends on the other variables, so adding or removing a variable changes it. Also, the computational requirements do not scale well with the dimension d , making this approach infeasible for ultrahigh dimensions.

So, if we want to be able to deal with high-dimensional data we do need to preserve some form of the product-moment technology. This leads us almost unavoidably to the

basic idea underlying Spearman’s rank correlation, which is to transform the variables first and then to compute product moments. We do not wish to restrict ourselves to ranks however, and we want to explore how far the principle of robustness by data transformation can be pushed.

In general, we consider a transformation g applied to the individual variables, and we define the resulting g -product moment as

$$\text{PM}_g(X_n, Y_n) := \text{PM}(g(X_n), g(Y_n)) \tag{7}$$

and similarly for Cov_g and Cor_g . Choosing $g(x_i) = x_i$ yields the usual product moment, and setting $g(x_i)$ equal to its rank yields the Spearman correlation. The g -product moment approach satisfies all three desired properties. First of all, if we use a bounded function g the population version $E[g(X)g(Y)]$ always exists and Cov_g satisfies the independence property without any moment conditions. Secondly, the resulting matrices always satisfy the PSD property. And finally, this method is very fast provided the transformation g can be computed quickly (which could be done in parallel over variables).

The remaining question, which will be addressed below, is whether we can find transformations g that yield covariances and correlations that are sufficiently robust and at the same time sufficiently efficient in the statistical sense. Our answer is affirmative.

The remainder of the paper is organized as follows. In section 2 we explore the properties of our g -product moment approach by means of influence functions, breakdown values and other robustness tools, designing some new transformations g based on what we have learned. Section 3 compares these transformations in a simulation study and makes recommendations. Section 4 explains how to use the method in higher dimensions, illustrated on some real high-dimensional data sets in Section 5.

2 Statistical properties

Note that the g -product moment $\text{PM}_g(X_j, X_k)$ between two variables X_j and X_k in a multivariate data set does not depend on the other variables, so we can study its properties in the bivariate setting.

The oldest type of robust g -product moments occur in rank correlations. Let us define a rescaled version of the sample ranks as $R_n(x_i) = (\text{Rank}(x_i) - 0.5)/n$ where $\text{Rank}(x_i)$ denotes the rank of x_i in $\{x_1, \dots, x_n\}$. The population version of $R_n(x_i)$ is the cumulative distribution function $F_X(x_i)$. Then the following functions g define well-known rank correlations:

- $g(x_i) = R_n(x_i)$ yields the Spearman rank correlation (Spearman, 1904);
- $g(x) = \text{sign}(R_n(x_i) - 0.5)$ gives the quadrant correlation (Mosteller, 1946);
- $g(x) = \Phi^{-1}(R_n(x))$ (where Φ is the standard gaussian cdf) yields the normal scores correlation, see e.g. Hájek and Sidak (1967).

Kendall's tau (Kendall, 1938) is of a somewhat different type as it replaces each variable X_n by a variable with $n(n-1)/2$ values, but we will compare with it later. If we want to use these rank transformations for covariance measures we have to take the scales of the original variables into account. Alqallaf et al. (2002) and Öllerer and Croux (2015) do this by multiplying the rank correlation by the product $\hat{\sigma}(X_n)\hat{\sigma}(Y_n)$ where $\hat{\sigma}$ is a robust scale estimator like the median absolute deviation (MAD) given by $\text{MAD}(X_n) = 1.4826 \text{median}_i |x_i - \text{median}_j(x_j)|$.

A second type of robust g -product moments goes back to Section 8.3 in the book of Huber (1981) and is based on M-estimation. Huber transforms x_i to

$$g(x_i) = \psi((x_i - \hat{\mu})/\hat{\sigma}) \tag{8}$$

where $\hat{\sigma}$ is a robust scale estimator such as the MAD, and $\hat{\mu}$ is an M-estimator of location given by the function ψ so that $\sum_i \psi((x_i - \hat{\mu})/\hat{\sigma}) = 0$. Note that $(x_i - \hat{\mu})/\hat{\sigma}$ is like a z-score but based on robust analogs of the mean and standard deviation. For $\psi(z) = \text{sign}(z)$ this yields $\hat{\mu} = \text{median}_j(x_j)$ so we recover the quadrant correlation. A more promising transformation is Huber's ψ_b function given by

$$\psi_b(z) = [z]_{-b}^b \tag{9}$$

for a given corner point $b > 0$, where the notation $[y]_a^b := \min(b, \max(a, y))$ stands for truncation. Another option is the sigmoid transformation $\psi(z) = \tanh(z)$. Note that the

transformation (8) does not require any tie-breaking rules, unlike the rank correlations. Huber (1981) derived the asymptotic efficiency of the ψ -product moment. We will go further by also computing the influence function, the breakdown value and other robustness measures. Our goal is to find a function ψ that is well-suited for correlation.

2.1 Influence function and efficiency

For analyzing the statistical properties of the ψ -product moment we assume a simple model for the ‘clean’ data, before outliers are added. The model says that (X, Y) follows a bivariate gaussian distribution F_ρ given by

$$F_\rho = N \left(\begin{bmatrix} 0 \\ 0 \end{bmatrix}, \begin{bmatrix} 1 & \rho \\ \rho & 1 \end{bmatrix} \right) \quad (10)$$

for $-1 < \rho < 1$, so F_0 is just the bivariate standard gaussian distribution. We will restrict ourselves to odd functions ψ so that $E[\psi(X)] = 0 = E[\psi(Y)]$, and study the statistical properties of $T_n = \text{ave}_i \psi(x_i)\psi(y_i)$ with population version $T_\psi = E[\psi(X)\psi(Y)]$.

Let us start with the influence function (IF) of T_ψ . Following Hampel et al. (1986), the raw influence function of T_ψ at F_ρ is defined in any point (x, y) as

$$\text{IF}_{raw}((x, y), T_\psi, F_\rho) = \frac{\partial}{\partial \varepsilon} T_\psi((1 - \varepsilon)F_\rho + \varepsilon\Delta_{(x,y)})|_{\varepsilon=0} \quad (11)$$

where $\Delta_{(x,y)}$ is the probability distribution that puts all its mass in (x, y) . The IF quantifies the effect of a small amount of contamination in (x, y) on T_ψ . It is easily verified that $\text{IF}_{raw}((x, y), T_\psi, F_0) = \psi(x)\psi(y)$ which becomes xy for the nonrobust $\psi(z) = z$.

However, we cannot compare the raw influence function (11) across different functions ψ since T_ψ is not Fisher-consistent, that is, $T_\psi(F_\rho) \neq \rho$ in general. For non-Fisher-consistent statistics T we follow the approach of Rousseeuw and Ronchetti (1981) and Hampel et al. (1986) by defining

$$\xi(\rho) := T(F_\rho) \quad \text{and} \quad U(F) := \xi^{-1}(T(F)) \quad (12)$$

so U is Fisher-consistent, and putting

$$\text{IF}((x, y), T, F) := \text{IF}_{raw}((x, y), U, F) = \frac{\text{IF}_{raw}((x, y), T, F)}{\xi'(\rho)} . \quad (13)$$

Proposition 1. For the influence function of T_ψ at F_0 we obtain $\xi'(0) = E[\psi']^2$ hence

$$IF((x, y), T_\psi, F_0) = \frac{\psi(x)\psi(y)}{E[\psi']^2}. \quad (14)$$

The proof can be found in section A.1 of the Additional Material.

Since the IF measures the effect of outliers we want it to be bounded, so we prefer bounded ψ unlike the classical choice $\psi(z) = z$. Note that (14) equals the raw influence function of $T^* = E[\psi^*(X)\psi^*(Y)]$ at F_0 where $\psi^*(u) = \psi(u)/E[\psi']$. When ψ is bounded T^* is integrable, so by the law of large numbers T_n^* is strongly consistent for its functional value: $T_n^* = \frac{1}{n} \sum_{i=1}^n \psi^*(x_i)\psi^*(y_i) \xrightarrow{a.s.} T^*(F_\rho)$ for $n \rightarrow \infty$. By the central limit theorem, T^* is then asymptotically normal under F_0 :

$$\sqrt{n}(T_n^* - 0) \rightarrow N(0, V)$$

where

$$V = \frac{E[\psi^2]^2}{E[\psi']^4} = \left(\frac{E[\psi^2]}{E[\psi']^2} \right)^2. \quad (15)$$

The classical method with $\psi(z) = z$ yields the lowest V , namely 1. Therefore, we obtain the asymptotic efficiency $\text{eff} = (E[\psi']^2/E[\psi^2])^2$. The asymptotic variance for $\rho \neq 0$ is determined in section A.2 in the Additional Material.

Note that the influence function of T_ψ at F_0 factorizes as the product of the influence functions of the M-estimator L_ψ of location with the same ψ -function:

$$IF((x, y), T_\psi, F_0) = IF(x, L_\psi, \Phi) IF(y, L_\psi, \Phi) . \quad (16)$$

This explains why the efficiency of T_ψ satisfies $\text{eff}(T_\psi) = (\text{eff}(L_\psi))^2$. We are also interested in attaining a low gross-error sensitivity $\gamma^*(T_\psi)$ which is defined as the supremum of $|IF((x, y), T_\psi, F_0)|$ and therefore equals $(\gamma^*(L_\psi))^2$. It follows from (Rousseeuw, 1981) that the quadrant correlation $\psi(z) = \text{sign}(z)$ has the lowest gross-error sensitivity among all statistics of the type $T_\psi = E[\psi(X)\psi(Y)]$. The quadrant correlation is said to be *most B-robust*, where the B refers to the **b**ias caused by outliers. In fact, $IF((x, y), T_\psi, F_0) = (\pi/2) \text{sign}(x) \text{sign}(y)$ yielding $\gamma_T^* = \pi/2$. However, the quadrant correlation is very inefficient as $\text{eff} = 4/\pi^2 = 40.5\%$.

On the other hand, from Hampel et al. (1986) it follows that the T_ψ based on Huber's ψ_b is *optimally B-robust*, which means that it is the most efficient among all ψ -functions with the same gross-error sensitivity $\gamma^*(T_\psi)$ as ψ_b .

The change-of-variance curve (Hampel et al., 1981; Rousseeuw, 1981) is given by

$$\text{CVC}(x, T_\psi, F) = \frac{\partial}{\partial \varepsilon} [\log V(T_\psi, (1 - \varepsilon)F + \varepsilon(\Delta_x + \Delta_{-x})/2)] \Big|_{\varepsilon=0} \quad (17)$$

and measures how stable the variance of the method is when the underlying distribution is contaminated. We do not want the variance to grow too much, as is measured by the change-of-variance sensitivity $\kappa^*(T_\psi)$ which is the supremum of the CVC. Since the asymptotic variance of T_ψ satisfies $V(T_\psi) = (V(L_\psi))^2$ we obtain $\text{CVC}(x, T_\psi, F_0) = 2 \text{CVC}(x, L_\psi, \Phi)$ and $\kappa^*(T_\psi) = 2 \kappa^*(L_\psi)$. Therefore we inherit all the results about the CVC. For instance, the quadrant correlation [with $\psi(z) = \text{sign}(z)$] is *most V-robust* (where V stands for variance) in that it has the lowest possible $\kappa^*(T_\psi)$. Also, the Huber ψ -function is *optimally V-robust* because it possesses the highest efficiency for a given $\kappa^*(T_\psi)$.

Now suppose that we do not want to assign any weight to outliers x that lie further away than a given distance c , that is, we impose

$$\psi(x) = 0 \quad \text{whenever} \quad |x| > c \quad . \quad (18)$$

Such functions ψ can no longer be monotone, and are called redescending instead. In the context of M-estimation of location, Hampel et al. (1981) showed that the optimally V-robust ψ -function satisfying (18), that is, the one with the highest efficiency subject to a given $\kappa^*(T_\psi)$, is of the following form:

$$\psi_{b,c}(z) = \begin{cases} z & \text{if } 0 \leq |z| \leq b \\ q_1 \tanh(q_2(c - |z|)) \text{sign}(z) & \text{if } b \leq |z| \leq c \\ 0 & \text{if } c \leq |z| \quad . \end{cases} \quad (19)$$

Here b is a corner point as in the Huber ψ_b . The constants q_1 and q_2 are such that the function $\psi_{b,c}$ is continuous. For any combination $0 < b < c$ the values of q_1 and q_2 can be derived as in section A.3 of the Additional Material. Our default choice will be $b = 1.5$ and $c = 4$, for which $q_1 = 1.540793$ and $q_2 = 0.8622731$. Note that the form of $\psi_{b,c}(z)$ for $b \leq |z| \leq c$ does not originate from Fisher's z , but is the result of solving a certain differential equation. The function $\psi_{b,c}$ yields the optimally V-robust T_ψ which rejects values that lie at least c robust standard deviations out.

A nice property of $\psi_{b,c}$ is that under normal circumstances a large majority of the data values (in fact 86.6% of them for $b = 1.5$) are left unchanged by the transformation, and only a minority is modified. It shares this property with the Huber transform but not with the common bisquare function. Leaving the majority of the data unchanged has the advantage that we keep much information about the distribution of a variable and the type of association between variables (e.g. linear), unlike rank transforms.

Interestingly, $\psi_{b,c}$ pushes values between b and c closer to the center so intermediate outliers still play some smaller role in the correlation, whereas far outliers do not count. For this reason we will refer to $\psi_{b,c}$ as our *wrapping function*, as it wraps the data around the interval $[-b, b]$. Indeed, the points on the interval are mapped to themselves, whereas the other points are wrapped around the corners, as in Figure 1.

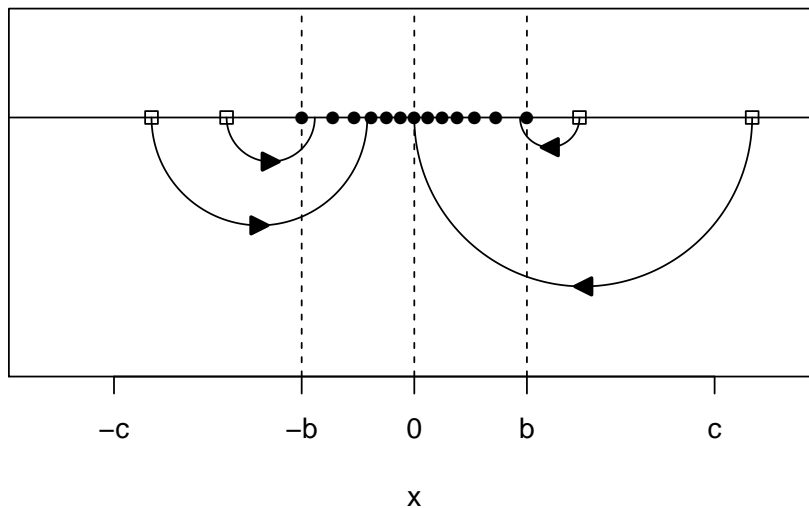


Figure 1: Illustration of wrapping a sample. Values in the interval $[-b, b]$ are left unchanged, whereas values outside $[-c, c]$ are zeroed. The intermediate values are ‘folded’ inward so they still play a role.

The influence functions of rank correlations were obtained by Croux and Dehon (2010) and Boudt et al. (2012). Note that for some rank correlations the function ξ of (12) is known explicitly, in fact $\xi(\rho) = \sin(\rho\pi/2)$ for the quadrant correlation, $\xi(\rho) = (6/\pi) \arcsin(\rho/2)$ for Spearman and $\xi(\rho) = \rho$ for normal scores. It turns out that these IF at F_0 match the expression in Proposition 1 if ψ corresponds to the population version of the transformation g in the rank correlation, as explained in Section A.4 of the Additional Ma-

terial. We can construct a truncated version of the normal scores correlation, given by $g(x) := \Phi^{-1}([R_n(x)]_\alpha^{1-\alpha})$. The truncated normal scores was first proposed on pages 210–211 of (Hampel et al., 1986) in the context of univariate rank tests. We can also truncate Spearman’s correlation by putting $g(x) := [R_n(x)]_\alpha^{1-\alpha}$.

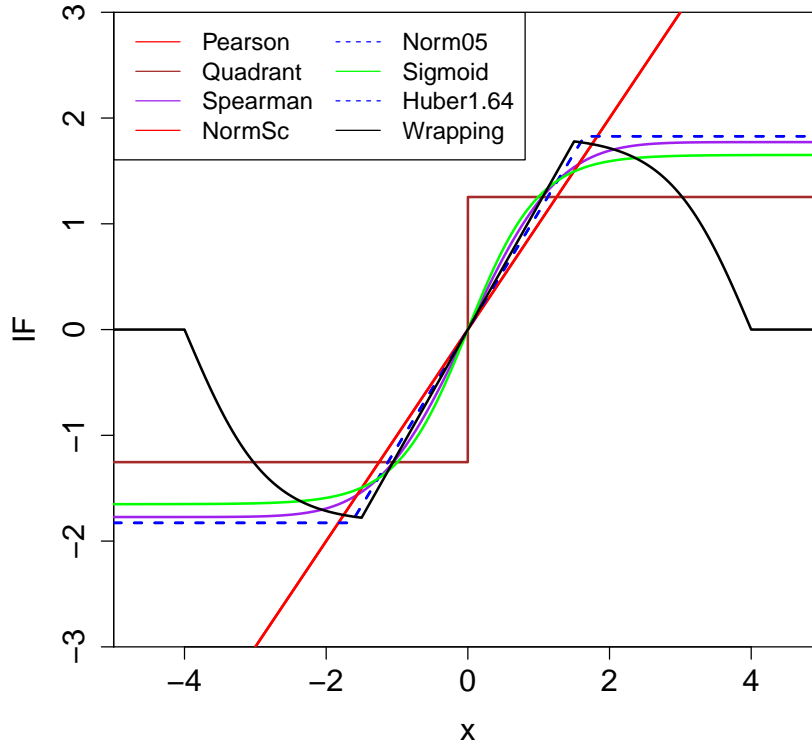


Figure 2: Location influence functions at $\rho = 0$ for different transformations g

The influence functions of rank correlations at F_0 also factorize as in (16). Figure 2 plots these location influence functions for several choices of the transformation g . We see that the Pearson and normal scores correlations have the same influence function (the identity) which is unbounded. On the other hand, the IF of Huber’s ψ_b stays constant outside the corner points $-b$ and b , whereas the IF of the wrapping function $\psi_{b,c}$ goes back to zero. The truncated normal scores has the same IF as Huber’s ψ_b provided $\alpha = \Phi(-b)$, so it is also optimally B-robust. The Spearman rank correlation and the sigmoid transformation have smooth influence functions.

2.2 Maximal bias and breakdown value

Whereas the IF measures the effect of one or a few outliers, we are now interested in the effect of a larger fraction ε of contamination. For the uncontaminated distribution of the bivariate (X, Y) we take the gaussian distribution $F = F_\rho$ given by (10). Then we consider all contaminated distributions of the form

$$F_{H,\varepsilon} = (1 - \varepsilon)F + \varepsilon H \quad (20)$$

where $\varepsilon \geq 0$ and H can be any distribution. This ε -contamination model is similar to the contaminated distributions in (11) and (17) but here H is more general.

A fraction ε of contamination can induce a maximum possible upward and downward bias on $T_\psi = \text{Cor}(\psi(X), \psi(Y))$ denoted by

$$B^+(\varepsilon, T_\psi, F) = \sup_{G \in \mathcal{F}_\varepsilon} (T_\psi(G) - T_\psi(F)) \quad \text{and} \quad B^-(\varepsilon, T_\psi, F) = \inf_{G \in \mathcal{F}_\varepsilon} (T_\psi(G) - T_\psi(F)) \quad (21)$$

where $\mathcal{F}_\varepsilon = \{G; G = (1 - \varepsilon)F + \varepsilon H \text{ for any distribution } H\}$. The proof of the following proposition is given in Section A.5 in the Additional Material.

Proposition 2. *Let $\varepsilon \in [0, 1]$ be fixed. Under the above conditions, the maximum upward bias is given by*

$$B^+(\varepsilon, T_\psi, F) = \frac{(1 - \varepsilon) \text{Var}_F(\psi(X)) T_\psi(F) + \varepsilon M^2}{(1 - \varepsilon) \text{Var}_F(\psi(X)) + \varepsilon M^2} - T_\psi(F) \quad (22)$$

with $M := \sup_x |\psi(x)|$, and the maximum downward bias is

$$B^-(\varepsilon, T_\psi, F) = \frac{(1 - \varepsilon) \text{Var}_F(\psi(X)) T_\psi(F) - \varepsilon M^2}{(1 - \varepsilon) \text{Var}_F(\psi(X)) + \varepsilon M^2} - T_\psi(F) . \quad (23)$$

The *breakdown value* ε^* of a robust estimator is loosely defined as the smallest ε that can make the result useless. For instance, a location estimator $\hat{\mu}$ becomes useless when its maximal bias tends to infinity. But correlation estimates stay in the bounded range $[-1, 1]$ hence the bias can never exceed 2 in absolute value, so the situation is not as clear-cut and several alternative definitions could be envisaged. Here we will follow the approach of Capéraà and Garralda (1997) who define the breakdown value of a correlation estimator as the smallest amount of contamination needed to give perfectly correlated variables a negative correlation. More precisely:

Definition 1. Let F be a bivariate distribution with $X = Y$, and R be a correlation measure. Then the breakdown value of R is defined as

$$\varepsilon^*(R) = \inf\{\varepsilon > 0 ; \inf_{G \in \mathcal{F}_\varepsilon} R(G) \leq 0\} .$$

The breakdown value of T_ψ then follows immediately from Proposition 2:

Corollary 1. The breakdown value ε^* of T_ψ equals

$$\varepsilon^*(T_\psi) = \frac{\text{Var}_F(\psi(X))}{\text{Var}_F(\psi(X)) + M^2} .$$

The breakdown values of rank correlations were obtained in (Capéraà and Garralda, 1997; Boudt et al., 2012). They used a different contamination model, but their results still hold under ε -contamination as explained in section A.6 in the Additional Material.

Table 1 lists some correlation measures based on transformations g that either use ranks or ψ -functions. For each the breakdown value ε^* and the efficiency and gross-error sensitivity γ^* at $\rho = 0$ are listed. The last column shows the product-moment correlation between a gaussian variable X and its transformed $g(X)$. The correlation is quite high for most transformations studied here, providing insight as to why this approach works.

In Table 1 we see that the quadrant correlation has the highest breakdown value but the lowest efficiency. The Spearman correlation reaches a much better compromise between breakdown and efficiency. Truncating the top 5% and bottom 5% of the ranks does not make much difference. Normal scores has the asymptotic efficiency and IF of Pearson but with a breakdown value of 12.4%, a nice improvement. Truncating 5% improves its robustness a bit at the small cost of 5% of efficiency, whereas truncating 10% brings its performance close to Spearman.

Note that the Huber correlation with $b = \Phi^{-1}(0.95)$ has the same IF as the 5% truncated normal scores correlation, and a higher ε^* . Lowering b to $\Phi^{-1}(0.90)$ yields a better breakdown value but lower efficiency. The same tradeoff holds for the corner point b of the wrapping function $\psi_{b,c}$.

Table 1: Correlation measures based on transformations g with their breakdown value ε^* , efficiency and gross-error sensitivity γ^* at $\rho = 0$, and correlation between X and $g(X)$.

Cor_g	ε^*	eff	γ^*	Cor
Pearson	0%	100%	∞	1
Quadrant	50%	40.5%	1.57	0.798
Spearman (SP)	20.6%	91.2%	3.14	0.977
Truncated SP, $\alpha = 0.05$	21.4%	89.0%	2.65	0.971
Truncated SP, $\alpha = 0.1$	23.5%	85.0%	2.32	0.960
Normal scores (NS)	12.4%	100%	∞	1
Truncated NS, $\alpha = 0.05$	16.3%	95.0%	3.34	0.987
Truncated NS, $\alpha = 0.1$	20.7%	88.9%	2.57	0.971
Sigmoid	28.3%	86.6%	2.73	0.965
Huber, $b = \Phi^{-1}(0.95) \approx 1.64$	23.5%	95.0%	3.34	0.987
Huber, $b = \Phi^{-1}(0.9) \approx 1.28$	29.2%	88.9%	2.57	0.971
Wrapping, $b = 1.5, c = 4$	25.1%	89.0%	3.16	0.971
Wrapping, $b = 1.3, c = 4$	28.1%	84.4%	2.79	0.958

3 Simulation Study

We now compare the correlation by transformation methods in Table 1 for finite samples. For the non rank-based methods we first normalize each variable by a robust scale estimate, and then estimate the location by the M-estimator with the given function ψ . Next we transform x_i to $x_i^* = \psi((x_i - \hat{\mu}_X)/\hat{\sigma}_X)$ and y_i to $y_i^* = \psi((y_i - \hat{\mu}_Y)/\hat{\sigma}_Y)$ and compute the plain Pearson correlation of the transformed sample $\{(x_1^*, y_1^*), \dots, (x_n^*, y_n^*)\}$.

Clean data. Let us start with uncontaminated data distributed as $F = F_\rho$ given by (10) where the true correlation ρ ranges over $\{0, 0.05, 0.10, \dots, 0.95\}$. For each ρ we generated $m = 5000$ bivariate data sets \mathbf{Z}^j with sample size $n = 100$. (We also generated data with $n = 20$ yielding the same qualitative conclusions.) We then estimate the bias

and the mean squared error (MSE) of each correlation measure R by

$$\text{bias}_\rho(R) = \text{ave}_{j=1}^m (R(\mathbf{Z}^j) - \rho) \quad \text{and} \quad \text{MSE}_\rho(R) = \text{ave}_{j=1}^m (R(\mathbf{Z}^j) - \rho)^2 . \quad (24)$$

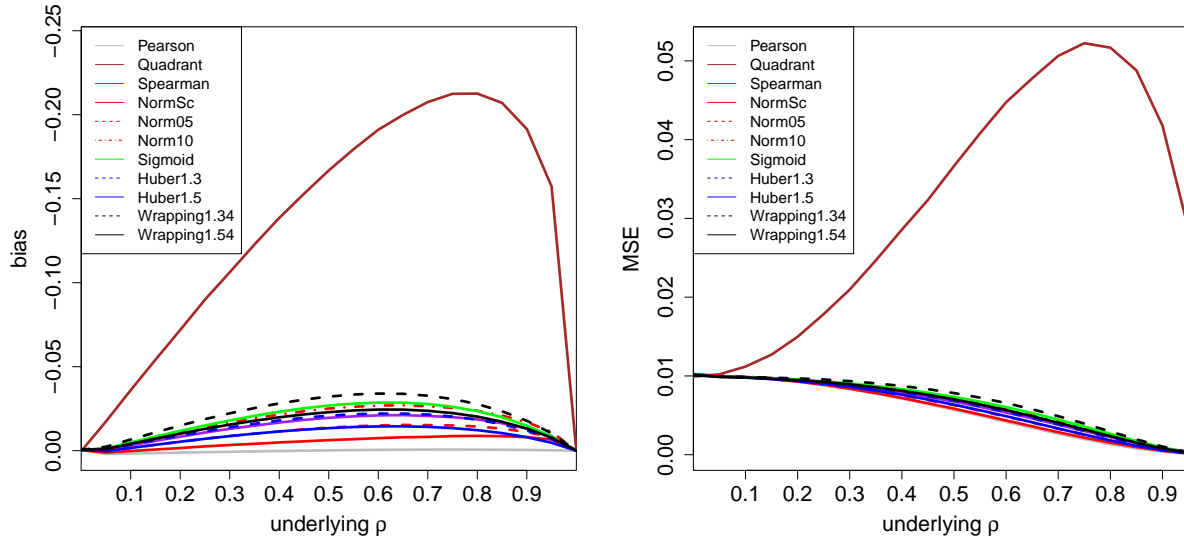


Figure 3: Bias and MSE of correlation measures based on transformation, for uncontaminated gaussian data with sample size 100.

The bias is shown in the left part of Figure 3. The vertical axis has flipped signs because the bias was always negative, so ρ is typically underestimated. Unsurprisingly, the Pearson correlation has the smallest bias (known not to be exactly zero). The normal scores correlation and the Huber ψ with $b = 1.5$ are fairly close, followed by truncated normal scores, Spearman and the sigmoid. Wrapping with $b = 1.5$ and $b = 1.3$ (both with $c = 4$) comes next, still with a fairly small bias. The bias of the quadrant correlation is much higher. Note that we could have reduced the bias of all of these methods by applying the consistency function ξ^{-1} of (12), which can be computed numerically. But such consistency corrections would destroy the crucial PSD property for the higher-dimensional data that motivate the present work, so we will not use them here.

The right panel of Figure 3 shows the MSE of the same methods, with a pattern similar to that of the bias. Even for $n = 25$ the bias dominated the variance (not shown).

Contaminated data. In order to compare the robustness of these correlation measures we now add outliers to the data. Since the true correlation ρ ranges over positive values

here, we will try to bring the correlation measures down. From the proof of Proposition 2 in section A.5 we know that the outliers have the biggest downward effect when placed at points $(k, -k)$ and $(-k, k)$ for some k . Therefore we will generate outliers from the distribution

$$H = \frac{1}{2}N\left(\begin{bmatrix} k \\ -k \end{bmatrix}, 0.01^2I\right) + \frac{1}{2}N\left(\begin{bmatrix} -k \\ k \end{bmatrix}, 0.01^2I\right)$$

for different values of k . The simulations were carried out for 10%, 20% and 30% of outliers, but we only show the results for 10% as the relative performance of the methods did not change much for the higher contamination levels.

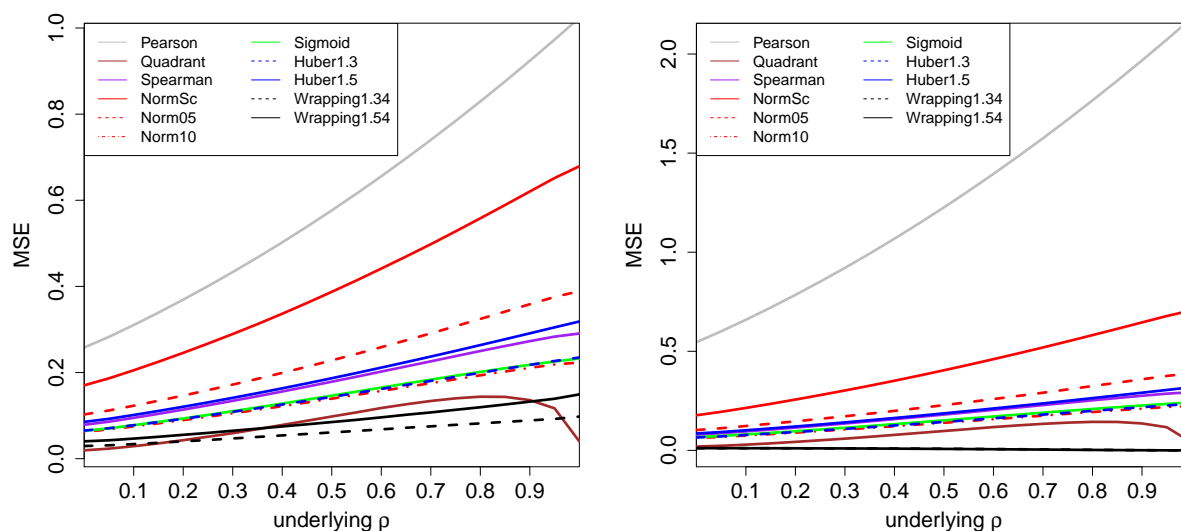


Figure 4: MSE of the correlation measures in Figure 3 with 10% of outliers placed at $k = 3$ (left) and $k = 5$ (right).

The results are shown in Figure 4 for $k = 3$ and $k = 5$. For $k = 3$ we see that the Pearson correlation has by far the highest MSE, followed by normal scores (whose breakdown value of 12.4% is not much higher than the 10% of contamination). The 5% truncated normal scores and the Huber with $b = 1.5$ do better, followed by the Spearman, the sigmoid, the 10% truncated normal scores and the Huber with $b = 1.3$. The quadrant correlation does best among all the methods based on a monotone transformation. However, wrapping still outperforms it, because it gives the outliers a smaller weight. Even though wrapping has a

slightly lower efficiency for clean data than Huber’s ψ_b with the same b , in return it delivers more resistance to outliers further away from the center.

For $k = 5$ the pattern is the same, except that the Pearson correlation is affected even more and wrapping has given a near-zero weight to the outliers. For $k = 2$ (not shown) the contamination is not really outlying and all methods performed about the same, whereas for $k > 5$ the curves of the non-Pearson correlations remain as they are for $k = 5$ since all transformations g are constant in that region.

Comparison with other robust correlation methods. As briefly described in the introduction, several good robust alternatives to the Pearson correlation exist that do not fall in our framework. We would like to find out how well wrapping stacks up against the most well-known of them, such as Kendall’s tau. We also compare with the Gnanadesikan-Kettenring (GK) approach (5) in which we replace the variance by the square of a robust scale, in particular the MAD and the scale estimator Q_n of Rousseeuw and Croux (1993) as studied by Ma and Genton (2001). For the approach starting with the estimation of a robust covariance matrix we consider the Minimum Covariance Determinant (MCD) method (Rousseeuw, 1985) using the algorithm in (Hubert et al., 2012), and the Spatial Sign Covariance Matrix (SSCM) of Visuri et al. (2000). In both cases we compute a correlation measure between variables X_1 and X_2 from the estimated scatter matrix C by (6). Note that the GK approach does not satisfy the PSD condition, and neither do the MCD and SSCM approaches when all $R(X_j, X_k)$ are computed from 2 variables only and are then plugged into a $d \times d$ matrix. Alternatively we could compute the MCD and SSCM in all d dimensions (ignoring computation time). To illustrate this we computed the MCD and the SSCM also in $d = 10$ dimensions where the true covariance matrix is given by $\Sigma_{jk} = \rho$ for $j \neq k$ and 1 otherwise. The simulation then reports the result of (6) on the first two variables only, ignoring the others.

The left panel of Figure 5 shows the bias of all these methods, in the same setting as Figure 3. The two GK methods and both MCD versions have the smallest bias, followed by wrapping. The Kendall bias is substantially larger, and in fact looks similar to the bias of the quadrant correlation in Figure 5, which is not so surprising since they possess the same function $\xi(\rho) = 2 \arcsin(\rho)/\pi$ in (12). The bias of the SSCM is even larger, both

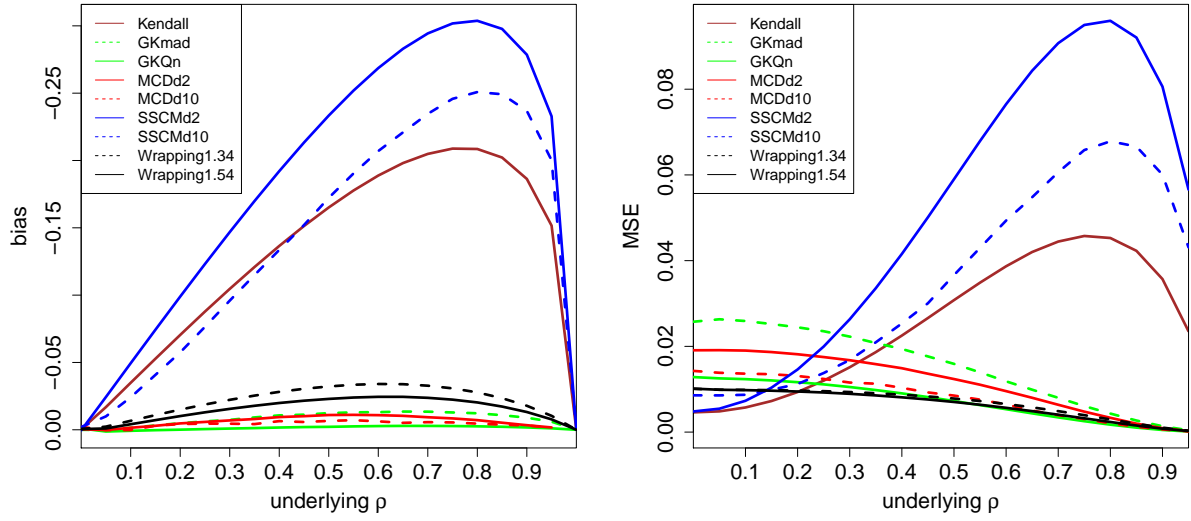


Figure 5: Bias and MSE of other robust correlation measures, for uncontaminated gaussian data with sample size 100.

when computed in $d = 2$ dimensions and in $d = 10$. The MSE in the right panel of Figure 5 shows a similar pattern.

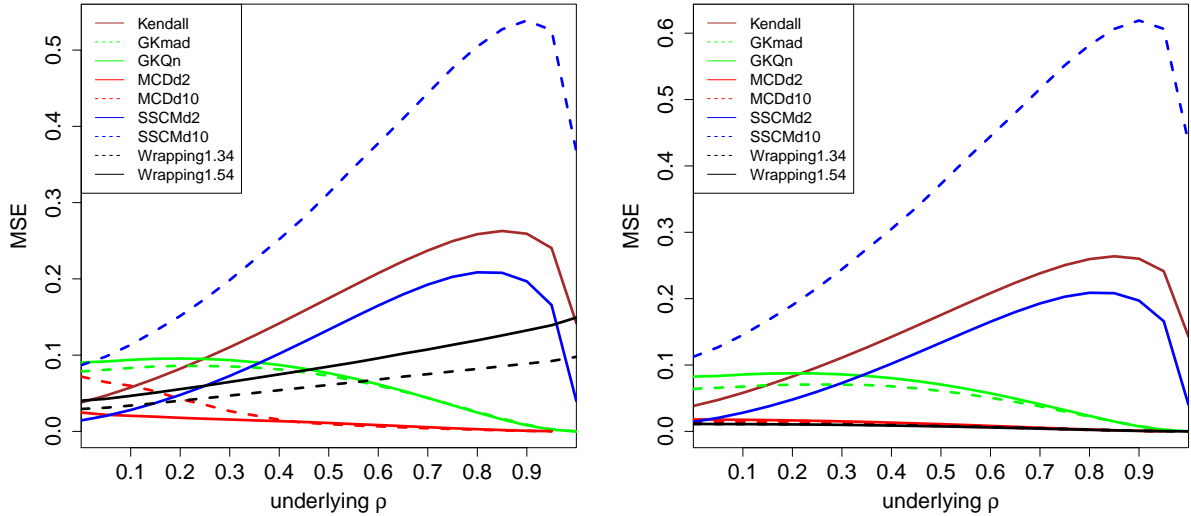


Figure 6: MSE of the correlation measures in Figure 5 with 10% of outliers placed at $k = 3$ (left) and $k = 5$ (right).

Figure 6 shows the effect of 10% of outliers, using the same generated data as in Figure

4. The left panel is for $k = 3$. The scale of the vertical axis indicates that the outliers have increased the MSE of all methods. The MCD in $d = 2$ dimensions is the least affected, whereas the GK methods, the SSCM with $d = 2$ and Kendall's tau are more sensitive. Note that the data in $d = 10$ dimensions was only contaminated in the first 2 dimensions, and the MCD still does quite well in that setting. On the other hand, the MSE of the SSCM in $d = 10$ is now much higher.

To conclude, wrapping holds its own even among well-known robust correlation measures outside our transformation approach. Perhaps surprisingly it substantially outperformed the SSCM, which was its main competitor in terms of computation speed and simplicity. Wrapping was not the overall best method in our simulation, that would be the MCD, but the latter requires much more computation time and that time goes up a lot in higher dimensions. Also note that the pairwise correlations obtained by the GK methods, the MCD and the SSCM lose the PSD property which necessitates an additional step, e.g. along the lines of Visuri et al. (2000), Ma and Genton (2001) and Maronna and Zamar (2002). Moreover, the highly robust quadrant transformation yields a low efficiency as it ignores much information in the data.

Therefore, wrapping seems a good choice for our purpose, which is to construct fast robust methods for fitting high dimensional data. This is not to say that it is the best for lower dimensional data, it most certainly is not, but the alternative methods do not extend easily to high dimensions or do not work as well in that setting.

4 Use in higher dimensions

4.1 Methodology

A large number if not the majority of multivariate analyses is based on product moments. Our approach is basically to wrap the data first, carry out an existing estimation technique on the wrapped data, and then use that fit for the original data. We proceed along the following steps.

Step 1: estimation. For each of the (possibly many) continuous variables X_j with $j = 1, \dots, d$ we compute a robust initial scale estimate $\hat{\sigma}_j$ such as the MAD. Then we

compute $\hat{\mu}_j$ by the location M-estimator with the wrapping function $\psi_{b,c}$ with defaults $b = 1.5$ and $c = 4$. This estimator can be iterated to convergence, but for speed we will typically take only 1 or 2 steps. The output of this step are the $(\hat{\mu}_j, \hat{\sigma}_j)$ for all j .

Step 2: transformation. Next we wrap the continuous variables. That is, we transform any x_{ij} to

$$x_{ij}^* = g(x_{ij}) = \hat{\mu}_j + \hat{\sigma}_j \psi_{b,c}\left(\frac{x_{ij} - \hat{\mu}_j}{\hat{\sigma}_j}\right) . \quad (25)$$

Note that $\text{ave}_i(x_{ij}^*)$ is a robust estimate of μ_j (in fact $\text{ave}_i(x_{ij}^*) = \hat{\mu}_j$ if the M-estimator in Step 1 was iterated to convergence), and $\text{stdev}_i(x_{ij}^*)$ is a robust estimate of σ_j . The wrapped variables X_j^* do not contain outliers, and when the original X_j is gaussian over 86% of its values remain unchanged, that is $x_{ij}^* = x_{ij}$.

What do we do when the data has missing values? If x_{ij} is NA and the method in Step 3 cannot handle NA's we have to assign a value to $g(x_{ij})$ in order to preserve the PSD property of product moment matrices, and $g(x_{ij}) = \mu_j$ is a natural choice. An alternative is multiple imputation if the size of the data set allows it. If Step 3 can deal with NA's, such as the EM algorithm for a covariance matrix, we can put $g(x_{ij}) = \text{NA}$. In that situation one can even put $g(x_{ij}) = \text{NA}$ for far outliers x_{ij} as was done by Agostinelli et al. (2015).

Note that we do not transform discrete variables. Depending on the context one may or may not leave them out of the subsequent analysis.

Step 3: fitting. We then fit the wrapped data x_{ij}^* by an existing multivariate method, yielding for instance a covariance matrix or sparse loading vectors.

Step 4: using the fit. To evaluate the fit we will look at the deviations (e.g. Mahalanobis distances) of the wrapped cases \mathbf{x}_i^* as well as the original cases \mathbf{x}_i .

Note that the time complexity of Steps 1 and 2 together is at most $O(n \log(n)d)$. As any multivariate method in Step 3 must read the data its complexity is at least $O(nd)$ and usually much higher, wrapping does not increase the complexity of the combined method.

4.2 Cellwise outliers

The coordinatewise approach in Steps 1 and 2 makes it especially robust against cellwise outliers, that is, deviating cells x_{ij} in the data matrix. In this paradigm a few cells in a row (case) can be anomalous whereas many other cells in the same row still contain useful

information, and in such situations we would rather not remove or downweight the entire row. The cellwise framework was first proposed and studied by Alqallaf et al. (2002, 2009).

Most robust techniques developed in the literature aim to protect against rowwise outliers. Such methods tend not to work well in the presence of cellwise outliers, because even a relatively small percentage of outlying cells may affect a large percentage of the rows. For this reason several authors have started to develop cellwise robust methods, see e.g. Agostinelli et al. (2015) and Rousseeuw and Van den Bossche (2018).

In the bivariate simulation of Section 3 we generated rowwise outliers, but the results for cellwise outliers are similar as seen in Section A.7 in the Additional Material.

4.3 Specific multivariate techniques

Covariance matrices. Computing the covariance between two wrapped variables yields

$$C(j, k) = \text{Cov}(X_j^*, X_k^*) = \hat{\sigma}_j \hat{\sigma}_k \text{Cor} \left(\psi_{b,c} \left(\frac{x_{ij} - \hat{\mu}_j}{\hat{\sigma}_j} \right), \psi_{b,c} \left(\frac{y_{ik} - \hat{\mu}_k}{\hat{\sigma}_k} \right) \right). \quad (26)$$

The resulting matrix is clearly PSD. We also have the independence property: if variables X_j and X_k are independent so are $X_j^* = g(X_j)$ and $X_k^* = g(X_k)$, and as these are bounded their population covariance exists and is zero.

Öllerer and Croux (2015) defined robust covariances with a formula like (26) in which the correlation on the right was a rank correlation. They showed that the explosion breakdown value of the resulting scatter matrix is at least that of the univariate scale estimator S yielding $\hat{\sigma}_j$ and $\hat{\sigma}_k$, and their proof goes through without changes in our setting. Therefore, the resulting robust covariance matrix has an explosion breakdown value of 50% which is higher than the values in Table 1.

The scatter matrix given by (26) is easy to compute and can be used as a part of other multivariate methods such as robust Mahalanobis distances for outlier detection, canonical correlation analysis etc. It can also serve as a fast initial estimate in the computation of other methods such as (Hubert et al., 2012).

Factor analysis. This technique is based on the covariance matrix of the variables, which can be replaced by the robust covariance matrix above.

Precision matrices and graphical models. The precision matrix is the inverse of the covariance matrix, and allows to construct a gaussian graphical model of the variables.

Liu et al. (2012), Öllerer and Croux (2015) and Tarr et al. (2016) estimated the covariance matrix from rank correlations, but one could also use wrapping for this step. When the dimension d is too high the covariance matrix cannot be inverted, so these authors construct a sparse precision matrix by applying the GLASSO (Friedman et al., 2008). Öllerer and Croux (2015) show that the breakdown value of the resulting precision matrix, for both implosion and explosion, is as high as that of the univariate scale estimator. This remains true for wrapping, so the resulting robust precision matrix has breakdown value 50% which is the highest possible.

Principal components. One way to construct a robust PCA is to first compute the covariance matrix of the wrapped variables as above, and then to carry out a spectral decomposition of this matrix. However, the number of pairwise covariances that need to be computed is $O(d^2)$, which is time-consuming in very high dimensions and may yield a matrix too large to store in memory. A better approach giving identical results is to perform a singular value decomposition (SVD) of the wrapped data set of size $n \times d$. Usually one only wants the main eigenvectors and then a reduced SVD suffices, saving more time.

Note that the resulting loadings can be used for the wrapped cases \mathbf{x}_i^* as well as the original cases \mathbf{x}_i . If desired also a sparse PCA can be carried out on the wrapped data.

Representing variables as points. The product moment technology allows for many nice mathematical shortcuts. For instance, let us standardize the column vectors (variables) $X_n = (x_1, \dots, x_n)^T$ and Y_n to zero mean and unit standard deviation. Then it is easy to verify that their correlation satisfies

$$\text{Cor}(X_n, Y_n) = \frac{1}{n-1} \langle X_n, Y_n \rangle = 1 - \frac{\|X_n - Y_n\|^2}{2(n-1)} \quad (27)$$

where $\|\dots\|$ is the usual euclidean distance. This monotone decreasing relation between correlation and distance allows us to switch from looking for high correlations in d dimensions to looking for small distances in n dimensions. When $d \gg n$ this is very helpful, and used e.g. in Google Correlate (Vanderkam et al., 2013).

The identity (27) can be exploited for robust correlation by wrapping the variables first. In the (ultra)high dimensional case we can then transpose our dataset so it becomes $d \times n$. If needed we can reduce the dimension even more to some $q \ll n$ by computing the main principal components as described before and projecting on them, which preserves their

euclidean distances to a large extent. This may allow visualization when q is small.

Classification of variables. One often has to classify a large number of variables, such as genes. When classifying the d wrapped variables we can represent them as d points in $q < n$ dimensions, and apply any of the available techniques for supervised classification such as linear and quadratic discriminant analysis and k -nearest neighbors. When a new variable (e.g. a stock trading on the same days) is to be classified, it first has to be wrapped.

For unsupervised classification several distance-based methods can then be used, such as k -means, k -medoids or agglomerative nesting, see e.g. (Kaufman and Rousseeuw, 1990).

5 Real data examples

Detecting outlying cells is not trivial because the correlation between the variables plays a role. The DetectDeviatingCells (DDC) method of Rousseeuw and Van den Bossche (2018) predicts the value of each cell from the columns strongly correlated with that cell's column. The original implementation of DDC required computing all $O(d^2)$ robust correlations between the d variables, yielding total time complexity $O(nd^2)$ which becomes prohibitive in ultrahigh dimensions.

However, we just saw how to represent wrapped variables as points. Finding the k variables that are most correlated to a variable X_j therefore comes down to finding its k nearest neighbors in q -dimensional space. Fortunately there exist fast approximate nearest neighbor algorithms (Arya et al., 1998) that can obtain the k nearest neighbors of all d points in q dimensions in $O(qd \log(d))$ time, a big improvement over $O(nd^2)$. Note that we want to find both large positive and large negative correlations, so we look for the k nearest neighbors in the set of all variables and their sign-flipped versions.

As an example, Singh et al. (2002) investigated the prediction of two different types of prostate cancer from genomic information. The data is available as the R file `Singh.rda` in <http://www.stats.uwo.ca/faculty/aim/2015/9850/microarrays/FitMArray/data/> and contains 12600 genes. The training set consists of 102 patients and the test set has 34. There is also a response variable with the clinical classification, -1 for tumor and 1 for nontumor.

With the fast version of DDC we can now analyze the entire genetic data set with $n = 136$ and $d = 12600$, which would not have been possible before. This took 8 minutes

on a laptop. Of course, the DDC method does not know the response variable or which rows correspond to the training set. Out of the 136 rows 35 were flagged as outlying, corresponding to the test set and one other patient. The resulting cellmap of size 136×12600 is hard to visualize. Therefore we selected the 100 most outlying variables, i.e. those with the most flagged cells, yielding the cellmap in Figure 7. As always the flagged cells are colored red when the observed value (gene expression level) is higher than predicted, and blue when it is lower than predicted.

Genes in prostate data

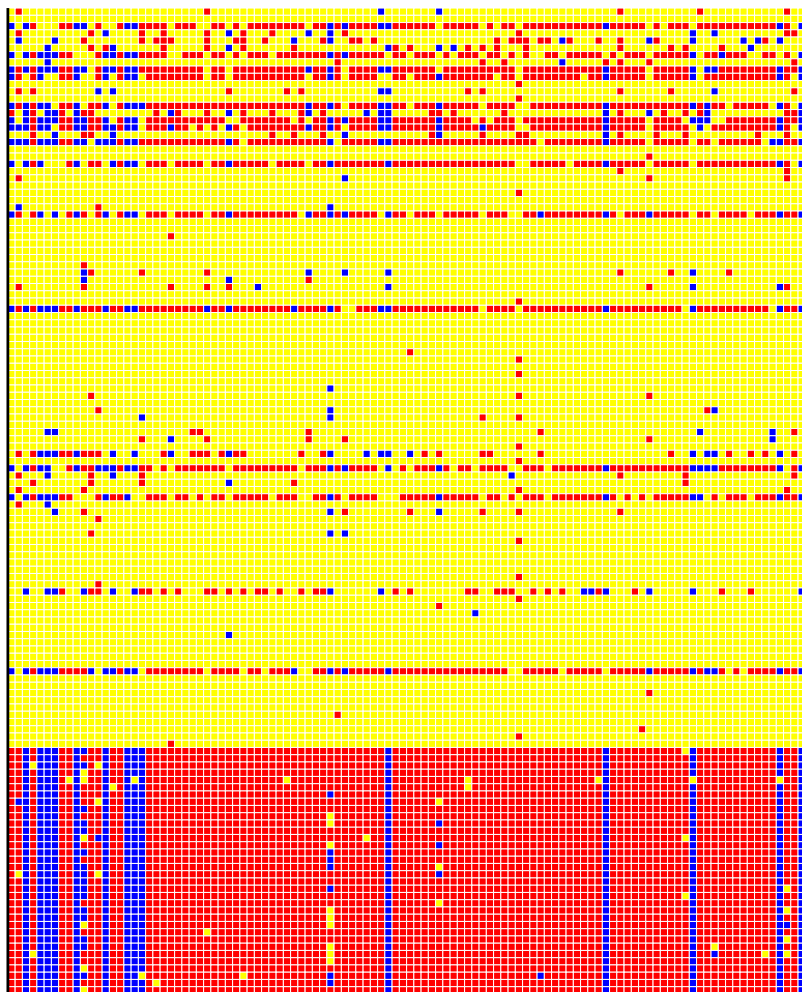


Figure 7: Prostate data: cellmap of the genes with the largest number of flagged cells.

The cellmap clearly shows that the bottom rows, corresponding to the test set, behave quite differently from the others. Indeed, it turns out that the test set was obtained by

a different laboratory. This indicates the need to align the training and test data sets by some form of standardization before using any model fitted on the training data to predict on the test data.

For our second example we analyze a video of a parking lot, filmed by a static camera. The raw video can be found on <http://imagelab.ing.unimore.it/visor> in the category *Videos for human action recognition in videosurveillance*. It was originally analyzed by Ballan et al. (2009) using sophisticated computer vision technology. The video is about 23 seconds long and consists of 230 Red/Green/Blue (RGB) frames of 640 by 480 pixels, so each frame corresponds with 3 matrices of size 640×480 . In the video we see two men coming from opposite directions, meeting in the center where they talk, and then running off one behind the other. The left part of Figure 9 shows 4 frames from the video. Note that every frame (case) is contaminated, but only in a minority of cells (pixels).

We treat the video as a dataset \mathbf{X} with 230 row vectors \mathbf{x}_i of length $921,600 = 640 \cdot 480 \cdot 3$, and we want to carry out a PCA based on the robust covariance between the 921,600 variables. When dealing with datasets this large one has to be careful with memory management, as a covariance matrix between these variables has nearly 10^{12} entries which is far too many to store in RAM memory. Therefore, we proceed as follows:

1. Wrap the 230 data values of each RGB pixel (column) X_j yielding the wrapped data matrix \mathbf{X}^* .
2. Compute the first $k = 3$ loadings of $\text{Cov}(\mathbf{X}^*) = \frac{n}{n-1} \text{PM}(\mathbf{X}^* - \overline{\mathbf{x}^*})$. We cannot actually store this covariance matrix, so instead we perform a singular value decomposition (SVD) of $\mathbf{X}^* - \overline{\mathbf{x}^*}$ with $k = 3$ components, which is mathematically equivalent. For this we use the efficient function `propack:svd()` from the R package `svd` with option `neig=3`, yielding the loading row vectors \mathbf{v}_j for $j = 1, 2, 3$. These correspond to principal images $\mathbf{v}_j + \overline{\mathbf{x}^*}$ that can be visualized.
3. Compute the 3-dimensional robust scores \mathbf{t}_i by projecting the *original* data on the robust loadings obtained from the *wrapped* data, i.e. $\mathbf{t}_i = (\mathbf{x}_i - \overline{\mathbf{x}^*})(\mathbf{v}_1^T, \mathbf{v}_2^T, \mathbf{v}_3^T)$.

A nonrobust analog of this procedure is to carry out steps 2 and 3 on $\mathbf{X} - \overline{\mathbf{x}}$ without any wrapping. Figure 8 shows the first principal image obtained by the nonrobust and



Figure 8: Parking lot video: first loading vector (image) of classical PCA (left) and of robust PCA (right).

the robust method. The images are similar, but in the nonrobust one we see two ‘ghosts’ standing in the center where the two men spent the most time, indicating that the classical PCA was attracted by this contamination. These ghosts do not appear in the robust principal image on the right, which was unaffected by the contamination. The same holds for the second and third principal images of both methods (not shown).

We can now compute a robust fit to each frame as $\hat{\mathbf{x}}_i = \mathbf{t}_i (\mathbf{v}_1^T, \mathbf{v}_2^T, \mathbf{v}_3^T)^T + \overline{\mathbf{x}^*}$. The residual of the frame is then $\mathbf{r}_i = \mathbf{x}_i - \hat{\mathbf{x}}_i$ whose 921,600 components (pixels) we can normalize by their robust scale. In the right panels of Figure 9 we see the part of the images on the left where the absolute normalized residuals exceed a threshold. These images only contain the men. In conclusion, this conceptually simple method has succeeded in accurately separating the movements from the background.

The entire analysis of this huge dataset of size 1.6 Gb in R took about two minutes on a laptop. Of course, in real-time situations one would estimate the robust loadings on an initial set of, say, 100 frames and then process new images while they are recorded, which is very fast as it only requires a matrix multiplication. In parallel with this the robust loadings can be updated from time to time.



Figure 9: Parking lot video. Left: frames 20, 60, 100 and 200. Right: their residual images.

6 Software availability

The wrapping transform is implemented in the R package *cellWise* on CRAN, which now also provides the faster version of DDC used in the first example. The package contains two vignettes with examples. The video data of the second example, its analysis and the video with results can be downloaded from <https://wis.kuleuven.be/stat/robust/software>.

7 Conclusions

High dimensional data often contain outlying (anomalous) values, so one needs robust methods that can detect and accommodate such outliers. It is not easy to construct methods that simultaneously satisfy the independence property, yield positive semidefinite matrices, and scale well with the dimension. We achieve this by transforming the data first, after which the usual methods based on product moments are applied.

Based on statistical properties such as the influence function, the breakdown value and efficiency we have selected a particular transform called wrapping. It leaves over 85% of the data intact under normality, which preserves partial information about the data distribution, granularity, and the shape of the relation between variables. Wrapping performs remarkably well in simulation even when compared with several well-known methods that are more computationally intensive. It is especially robust against cellwise outliers.

References

- Agostinelli, C., A. Leung, V. J. Yohai, and R. H. Zamar (2015). Robust estimation of multivariate location and scatter in the presence of cellwise and casewise contamination. *Test* 24(3), 441–461.
- Alqallaf, F., K. Konis, R. D. Martin, and R. H. Zamar (2002). Scalable robust covariance and correlation estimates for data mining. In *Proceedings of the Eighth ACM SIGKDD International Conference on Knowledge Discovery and Data Mining, KDD '02*, New York, NY, USA, pp. 14–23. ACM.

- Alqallaf, F., S. Van Aelst, V. J. Yohai, and R. H. Zamar (2009). Propagation of outliers in multivariate data. *The Annals of Statistics* 37(1), 311–331.
- Arya, S., D. M. Mount, N. S. Netanyahu, R. Silverman, and A. Y. Wu (1998). An optimal algorithm for approximate nearest neighbor searching fixed dimensions. *Journal of the ACM* 45(6), 891–923.
- Ballan, L., M. Bertini, A. Del Bimbo, L. Seidenari, and G. Serra (2009). Effective codebooks for human action categorization. In *Proceedings of ICCV International Workshop on Video-oriented Object and Event Classification*, Kyoto, Japan, pp. 506–513.
- Boudt, K., J. Cornelissen, and C. Croux (2012). The Gaussian rank correlation estimator: robustness properties. *Statistics and Computing* 22(2), 471–483.
- Capéraà, P. and A. I. Garralda (1997). Taux de résistance des tests de rang d’indépendance. *The Canadian Journal of Statistics* 25(1), 113–124.
- Croux, C. and C. Dehon (2010). Influence functions of the Spearman and Kendall correlation measures. *Statistical Methods & Applications* 19(4), 497–515.
- Ferguson, T. (1996). *A Course in Large Sample Theory*. Chapman & Hall Texts in Statistical Science Series. Taylor & Francis.
- Friedman, J., T. Hastie, and R. Tibshirani (2008). Sparse inverse covariance estimation with the graphical lasso. *Biostatistics* 9, 432–441.
- Gnanadesikan, R. and J. Kettenring (1972). Robust estimates, residuals, and outlier detection with multiresponse data. *Biometrics* 28, 81–124.
- Hájek, J. and Z. Sidak (1967). *Theory of Rank Tests*. New York: Academic Press.
- Hampel, F., E. Ronchetti, P. J. Rousseeuw, and W. Stahel (1986). *Robust Statistics: The Approach Based on Influence Functions*. New York: Wiley.
- Hampel, F., P. J. Rousseeuw, and E. Ronchetti (1981). The change-of-variance curve and optimal redescending M-estimators. *Journal of the American Statistical Association* 76, 643–648.

- Huber, P. (1981). *Robust Statistics*. New York: Wiley.
- Hubert, M., P. J. Rousseeuw, and T. Verdonck (2012). A deterministic algorithm for robust location and scatter. *Journal of Computational and Graphical Statistics* 21, 618–637.
- Kaufman, L. and P. J. Rousseeuw (1990). *Finding groups in data: An introduction to cluster analysis*. New York: Wiley.
- Kendall, M. G. (1938). A new measure of rank correlation. *Biometrika* 30(1/2), 81–93.
- Liu, H., F. Han, M. Yuan, J. Lafferty, and L. Wasserman (2012). High-dimensional semi-parametric gaussian copula graphical models. *The Annals of Statistics* 40, 2293–2326.
- Ma, Y. and M. G. Genton (2001). Highly robust estimation of dispersion matrices. *Journal of Multivariate Analysis* 78(1), 11 – 36.
- Maronna, R., D. Martin, and V. Yohai (2006). *Robust Statistics: Theory and Methods*. New York: Wiley.
- Maronna, R. and R. Zamar (2002). Robust estimates of location and dispersion for high-dimensional data sets. *Technometrics* 44, 307–317.
- Mosteller, F. (1946). On some useful "inefficient" statistics. *The Annals of Mathematical Statistics* 17(4), 377–408.
- Öllerer, V. and C. Croux (2015). Robust high-dimensional precision matrix estimation. In K. Nordhausen and S. Taskinen (Eds.), *Modern Nonparametric, Robust and Multivariate Methods: Festschrift in Honour of Hannu Oja*, pp. 325–350. Cham: Springer International Publishing.
- Rousseeuw, P. J. (1981). A new infinitesimal approach to robust estimation. *Zeitschrift für Wahrscheinlichkeitstheorie und Verwandte Gebiete* 56(1), 127–132.
- Rousseeuw, P. J. (1984). Least median of squares regression. *Journal of the American Statistical Association* 79, 871–880.

- Rousseeuw, P. J. (1985). Multivariate estimation with high breakdown point. In W. Grossmann, G. Pflug, I. Vincze, and W. Wertz (Eds.), *Mathematical Statistics and Applications, Vol. B*, pp. 283–297. Dordrecht: Reidel Publishing Company.
- Rousseeuw, P. J. and C. Croux (1993). Alternatives to the median absolute deviation. *Journal of the American Statistical Association* 88, 1273–1283.
- Rousseeuw, P. J. and E. Ronchetti (1981). Influence curves of general statistics. *Journal of Computational and Applied Mathematics* 7(3), 161–166.
- Rousseeuw, P. J. and W. Van den Bossche (2018). Detecting deviating data cells. *Technometrics*, to appear.
- Shevlyakov, G. and H. Oja (2016). *Robust Correlation: Theory and Applications*. New York: Wiley.
- Singh, D., P. Febbo, K. Ross, D. Jackson, J. Manola, C. Ladd, P. Tamayo, A. Renshaw, A. D’Amico, J. Richie, E. Lander, M. Loda, P. Kantoff, T. Golub, and W. Sellers (2002). Gene expression correlates of clinical prostate cancer behavior. *Cancer Cell* 1, 203–209.
- Spearman, C. (1904). General intelligence, objectively determined and measured. *The American Journal of Psychology* 15(2), 201–292.
- Tarr, G., S. Muller, and N. Weber (2016). Robust estimation of precision matrices under cellwise contamination. *Computational Statistics and Data Analysis* 93, 404 – 420.
- Vanderkam, S., R. Schonberger, H. Rowley, and S. Kumar (2013). *Nearest Neighbor Search in Google Correlate*. Google. <http://www.google.com/trends/correlate/nnsearch.pdf>.
- Visuri, S., V. Koivunen, and H. Oja (2000). Sign and rank covariance matrices. *Journal of Statistical Planning and Inference* 91, 557–575.

A Additional Material

Here the proofs of the results are collected.

A.1 Proof of Proposition 1

We can generate $(X, Y) \sim F_\rho$ for $\rho \geq 0$ by

$$\begin{bmatrix} X \\ Y \end{bmatrix} = A \begin{bmatrix} U \\ V \\ W \end{bmatrix},$$

where $U, V, W \sim N(0, 1)$ are i.i.d. and

$$A = \begin{bmatrix} \sqrt{1-\rho} & 0 & \sqrt{\rho} \\ 0 & \sqrt{1-\rho} & \sqrt{\rho} \end{bmatrix}.$$

We now obtain $\xi(\rho) = \int \psi(u\sqrt{1-\rho} + w\sqrt{\rho})\psi(v\sqrt{1-\rho} + w\sqrt{\rho})dN_{0,I}(u, v, w)$. Since we are interested in $\rho \approx 0$, we can use the Taylor expansion (derived with $\delta = \sqrt{\rho}$) to obtain $\psi(u\sqrt{1-\rho} + w\sqrt{\rho}) = \psi(u) + w\sqrt{\rho}\psi'(u) + \frac{w^2\rho}{2}\psi''(u) + o(\rho)$ and similarly for the second factor, yielding 9 terms of which only one term remains, the others being $o(\rho)$ or zero by asymmetry:

$$\begin{aligned} \xi(\rho) &= E \left[\psi(u) \left\{ \psi(v) + w\sqrt{\rho}\psi'(v) + \frac{w^2\rho}{2}\psi''(v) \right\} \right. \\ &\quad \left. + w\sqrt{\rho}\psi'(u) \left\{ \psi(v) + w\sqrt{\rho}\psi'(v) + \frac{w^2\rho}{2}\psi''(v) \right\} \right. \\ &\quad \left. + \frac{w^2\rho}{2}\psi''(u) \left\{ \psi(v) + w\sqrt{\rho}\psi'(v) + \frac{w^2\rho}{2}\psi''(v) \right\} \right] \\ &= \rho E [w^2\psi'(u)\psi'(v)] + o(\rho) \\ &= \rho E[\psi'(u)]E[\psi'(v)] + o(\rho) \end{aligned}$$

Therefore $\xi'(0) = E[\psi'(u)]^2$ and we obtain $\text{IF}((x, y), T, F_0) = \psi(x)\psi(y)/E[\psi']^2$.

A.2 Asymptotic distribution for general ρ

We now wish to compute the asymptotic distribution of $\text{PM}(\psi(X_n), \psi(Y_n))$ when (X, Y) has the normal distribution F_ρ given by (10) with $\rho \neq 0$. Denote $U = \psi(X)$ and $V = \psi(Y)$

with finite samples $U_n = \psi(X_n)$ and $V_n = \psi(Y_n)$. Since $|\psi(z)| \leq |z|$ for all functions ψ under consideration, the fourth moments of (U, V) are finite. We then apply the CLT and the delta method as in Theorem 8 on page 52 of (Ferguson, 1996), yielding

$$\sqrt{n}(\text{Cov}(U_n, V_n) - \text{Cov}(U, V)) \xrightarrow{D} N(0, A\Sigma^*A^T), \quad (\text{A.1})$$

where

$$A = \left(-\frac{\text{Cov}(U, V)}{2\text{Var}(U)}, -\frac{\text{Cov}(U, V)}{2\text{Var}(V)}, \frac{1}{\sqrt{\text{Var}(U)\text{Var}(V)}} \right) \quad (\text{A.2})$$

and

$$\Sigma^* = \begin{bmatrix} \text{Var}(U^2) & \text{Cov}(U^2, V^2) & \text{Cov}(U^2, UV) \\ \text{Cov}(V^2, U^2) & \text{Var}(V^2) & \text{Cov}(V^2, UV) \\ \text{Cov}(UV, U^2) & \text{Cov}(V^2, UV) & \text{Var}(UV) \end{bmatrix}.$$

For $\psi(z) = z$ this yields the well-known result $A\Sigma^*A^T = (1 - \rho^2)^2$. If ψ is not the identity the asymptotic variance does not necessarily allow an elegant expression, but can be computed numerically.

A.3 Construction of the optimal V-robust transformation

Theorem 3.1 in (Hampel et al., 1981) says that for any $0 < c < \infty$ and large enough $k > 0$ there exist positive constants $0 < b < c$, A and B such that $\tilde{\psi}$ defined by

$$\tilde{\psi}(z) = \begin{cases} z & \text{if } 0 \leq |z| \leq b \\ \sqrt{A(k-1)} \tanh\left(\frac{B}{2}\sqrt{\frac{k-1}{A}}(c-|z|)\right) \text{sign}(z) & \text{if } b \leq |z| \leq c \\ 0 & \text{if } c \leq |z| \end{cases} \quad (\text{A.3})$$

satisfies

$$b = \sqrt{A(k-1)} \tanh\left(\frac{1}{2}\sqrt{\frac{(k-1)B^2}{A}}(c-b)\right),$$

$A = \int_{-c}^c \tilde{\psi}(x)^2 d\Phi(x)$, $B = \int_{-c}^c \tilde{\psi}'(x) d\Phi(x)$ and $\kappa^*(\tilde{\psi}) = k$. Theorem 4.1 then says that this function $\tilde{\psi}$ minimizes the asymptotic variance among all odd functions ψ satisfying (18) subject to $\kappa^*(\psi) \leq k$, and that this optimal solution is unique (upto a positive nonzero factor). It can be verified that for a given value of c there is a strictly monotone relation between k and b , so we have decided to parametrize $\tilde{\psi}$ by the easily interpretable tuning

constants b and c . A short R-script is available that for any b and c derives the other constants A , B and k , in turn yielding $q_1 = \sqrt{A(k-1)}$ and $q_2 = (B/2)\sqrt{(k-1)/A}$. For instance, for $b = 1.5$ and $c = 4$ we obtain $A = 0.7532528$, $B = 0.8430849$ and $k = 4.1517212$ hence $q_1 = 1.540793$ and $q_2 = 0.8622731$, yielding the gross-error-sensitivity $(b/B)^2 = 3.16$ and the efficiency $(B^2/A)^2 = 0.890$.

A.4 Relation with influence functions of rank correlations

At the model distribution F_0 the influence functions of the Quadrant and Spearman correlation (Croux and Dehon, 2010) and the normal scores (Boudt et al., 2012) correspond to those of certain ψ -product moments. This is not a coincidence, because if we write the rank transform as $g(x_i) = h(R_n(x_i))$ it tends to the function $\tilde{g}(x) = h(\Phi(x))$ when $n \rightarrow \infty$. If we put $\psi(x) := h(\Phi(x))$ we observe that (16) indeed holds, with $\text{IF}(x, h, \Phi) = h(\Phi(x)) / \int (h(\Phi))' d\Phi = \psi(x) / E[\psi']$.

For the quadrant correlation $h(u) = \text{sign}(u - 1/2)$ we get the IF of the median:

$$\text{IF}(x, L_h, \Phi) = \frac{\text{sign}(x)}{2\Phi'(0)} = \sqrt{\frac{\pi}{2}} \text{sign}(x)$$

and so $\gamma^* = \pi/2$ and $\text{eff} = 4/\pi^2$.

For the normal scores rank correlation we have $h(u) = \Phi^{-1}(u)$ hence $\text{IF}(x, L_h, \Phi) = x$ which is the influence function of the mean and thus unbounded, yielding $\gamma^* = \infty$ and $\text{eff} = 1$. The truncated normal scores $h(u) = \Phi^{-1}([u]_\alpha^{1-\alpha}) = [\Phi^{-1}(u)]_{-b}^b$ where $\alpha = \Phi(-b)$ yields $\text{IF}(x, L_h, \Phi) = \psi_b(x) / E[\psi'_b]$, which is the influence function of Huber's ψ_b function. Therefore, the truncated normal scores correlation is also optimally B-robust.

For the Spearman correlation ($h(u) = u - 1/2$) we obtain

$$\text{IF}(x, L_h, \Phi) = \frac{\Phi(x) - 1/2}{E[(\Phi')^2]} = 2\sqrt{\pi} \left(\Phi(x) - \frac{1}{2} \right)$$

which is also the influence function of the Hodges-Lehmann estimator and the Mann-Whitney and Wilcoxon tests (Hampel et al., 1986). It yields $\gamma^* = \pi$ and $\text{eff} = 9/\pi^2$.

A.5 Proof of Proposition 2 and Corollary 1

Proof of Proposition 2. We give the proof for the maximum upward bias (the result for the maximum downward bias then follows by replacing Y by $-Y$). The uncontaminated

distribution of (X, Y) is $F = F_\rho$ from (10). Since $\psi(X)$ and $\psi(Y)$ have the same distribution and ψ is odd and bounded we find $E_F[\psi(X)] = E_F[\psi(Y)] = 0$ and $E_F[\psi(X)^2] = E_F[\psi(Y)^2]$. Now consider the contaminated distribution $G = (1-\varepsilon)F_\rho + \varepsilon H$ where H is any distribution. At G we obtain

$$\text{Cor}_G(\psi(X), \psi(Y)) = \frac{E_G[(\psi(X) - E_G[\psi(X)])(\psi(Y) - E_G[\psi(Y)])]}{\sqrt{E_G[(\psi(X) - E_G[\psi(X)])^2]E_G[(\psi(Y) - E_G[\psi(Y)])^2]}}$$

which works out to be

$$\frac{(1-\varepsilon)\text{Cov}_F(U, V) + \varepsilon E_H[UV] - \varepsilon^2 E_H[U]E_H[V]}{\sqrt{((1-\varepsilon)V_F + \varepsilon E_H[U^2] - \varepsilon^2 E_H[U]^2)((1-\varepsilon)V_F + \varepsilon E_H[V^2] - \varepsilon^2 E_H[V]^2)}} \quad (\text{A.4})$$

where we denote $U := \psi(X)$ and $V := \psi(Y)$ to save space, as well as $V_F := \text{Var}_F(U) = E_F[\psi(X)^2] = E_F[\psi(Y)^2] = \text{Var}_F(V)$.

We will show the proof for $\rho = 0$ which implies that U and V are independent hence $\text{Cov}_F(U, V) = 0$ as this reduces the notation, but the proof remains valid if the term $(1-\varepsilon)\text{Cov}_F(U, V) = (1-\varepsilon)V_F T_\psi(F)$ is kept. The proof consists of two parts. We first show that the contaminated correlation (A.4) is bounded from above by

$$C(\varepsilon) := \frac{\varepsilon M^2}{(1-\varepsilon)V_F + \varepsilon M^2} \quad (\text{A.5})$$

and then we provide a sequence of contaminating distributions H_n for which (A.4) tends to this upper bound.

1. Suppose first that $E_H[U]E_H[V] \leq 0$. Then we have for the numerator of (A.4):

$$\begin{aligned} E_H[UV] - \varepsilon E_H[U]E_H[V] &\leq E_H[UV] - E_H[U]E_H[V] \\ &\leq \sqrt{(E_H[U^2] - E_H[U]^2)(E_H[V^2] - E_H[V]^2)}. \end{aligned}$$

Now consider the denominator of (A.4) and note that

$$\begin{aligned} \sqrt{((1-\varepsilon)V_F + \varepsilon(E_H[U^2] - \varepsilon E_H[U]^2))((1-\varepsilon)V_F + \varepsilon(E_H[V^2] - \varepsilon E_H[V]^2))} &\geq \\ \sqrt{((1-\varepsilon)V_F + \varepsilon(E_H[U^2] - E_H[U]^2))((1-\varepsilon)V_F + \varepsilon(E_H[V^2] - E_H[V]^2))} & \end{aligned}$$

because $E_H[U^2] - E_H[U]^2 \geq 0$, $E_H[U^2] \geq 0$, $E_H[U]^2 \geq 0$ and $0 \leq \varepsilon \leq 1$. Therefore, we can bound (A.4) from above by

$$\frac{\varepsilon \sqrt{(E_H[U^2] - E_H[U]^2)(E_H[V^2] - E_H[V]^2)}}{\sqrt{((1-\varepsilon)V_F + \varepsilon(E_H[U^2] - E_H[U]^2))((1-\varepsilon)V_F + \varepsilon(E_H[V^2] - E_H[V]^2))}}$$

and this quantity is maximal when $(E_H[U^2] - \varepsilon E_H[U]^2)$ and $(E_H[V^2] - \varepsilon E_H[V]^2)$ are as large as possible. Their supremum is in fact M^2 . Therefore, (A.4) is less than or equal to (A.5).

2. Suppose now that $E_H[U]E_H[V] > 0$. We will first show that the numerator is bounded as follows:

$$E_H[UV] - \varepsilon E_H[U]E_H[V] \leq \sqrt{(E_H[U^2] - \varepsilon E_H[U]^2)(E_H[V^2] - \varepsilon E_H[V]^2)} . \quad (\text{A.6})$$

By squaring both sides we find that this is equivalent to showing

$$\begin{aligned} & E_H[UV]^2 - 2\varepsilon E_H[U]E_H[V]E_H[UV] \\ & \leq E_H[U^2]E_H[V^2] - \varepsilon(E_H[U^2]E_H[V]^2 + E_H[U]^2E_H[V^2]) \end{aligned}$$

which is equivalent to

$$E_H[U^2]E_H[V^2] - E_H[UV]^2 + \varepsilon(2E_H[U]E_H[V]E_H[UV] - E_H[U^2]E_H[V]^2 - E_H[U]^2E_H[V^2]) \geq 0. \quad (\text{A.7})$$

We know that (A.6) holds for $\varepsilon = 1$ as it is equivalent to $\text{Cov}_H(U, V) \leq \sqrt{\text{Var}_H(U) \text{Var}_H(V)}$ so (A.7) is true in that case.

The general version of (A.7) with $\varepsilon \leq 1$ equals the LHS for $\varepsilon = 1$, plus $(1 - \varepsilon)$ times

$$E_H[U]^2E_H[V^2] - 2E_H[U]E_H[V]E_H[UV] + E_H[U^2]E_H[V]^2 . \quad (\text{A.8})$$

Therefore, it would suffice to prove that (A.8) is nonnegative. We know that $|E_H[UV]| \leq \sqrt{E_H[U^2]E_H[V^2]}$ by Cauchy-Schwarz. Since $E_H[U]E_H[V] > 0$ we obtain

$$\begin{aligned} & E_H[U]^2E_H[V^2] - 2E_H[U]E_H[V]E_H[UV] + E_H[U^2]E_H[V]^2 \\ & \geq E_H[U]^2E_H[V^2] - 2E_H[U]E_H[V]\sqrt{E_H[U^2]E_H[V^2]} + E_H[U^2]E_H[V]^2 \\ & = \left(E_H[U]\sqrt{E_H[V^2]} - E_H[V]\sqrt{E_H[U^2]} \right)^2 \geq 0 . \end{aligned}$$

Now that we have shown (A.6) we can proceed as in part 1, since (A.4) is bounded from above by

$$\frac{\varepsilon \sqrt{(E_H[U^2] - \varepsilon E_H[U]^2)(E_H[V^2] - \varepsilon E_H[V]^2)}}{\sqrt{((1 - \varepsilon)V_F + \varepsilon(E_H[U^2] - \varepsilon E_H[U]^2))((1 - \varepsilon)V_F + \varepsilon(E_H[V^2] - \varepsilon E_H[V]^2))}}$$

and this quantity is maximal when $(E_H[U^2] - \varepsilon E_H[U]^2)$ and $(E_H[V^2] - \varepsilon E_H[V]^2)$ are as large as possible. Their supremum is again M^2 , so (A.4) is less than or equal to (A.5).

3. Now all that is left to show is that the upper bound (A.5) is sharp. Let $(k_n)_{n \in \mathbb{N}}$ be a sequence such that $\lim_{n \rightarrow \infty} \psi(k_n) = \sup_x |\psi(x)| = M$ and consider the sequence of ‘worst-placed’ contaminating distributions

$$H_n = \frac{1}{2} \Delta_{(k_n, k_n)} + \frac{1}{2} \Delta_{(-k_n, -k_n)} . \quad (\text{A.9})$$

For the numerator of (A.4) we have $\lim_{n \rightarrow \infty} \varepsilon E_{H_n}[UV] - \varepsilon^2 E_{H_n}[U] E_{H_n}[V] = \varepsilon M^2$ since $E_{H_n}[U] = 0 = E_{H_n}[V]$, and for the denominator we obtain analogously

$$\lim_{n \rightarrow \infty} \sqrt{((1 - \varepsilon) V_F + \varepsilon E_{H_n}[U^2])((1 - \varepsilon) V_F + \varepsilon E_{H_n}[V^2])} = (1 - \varepsilon) V_F + \varepsilon M^2$$

so we reach the upper bound (A.5). The proof for the maximum downward bias is entirely similar, and there the worst placed contaminating distributions are of the form $H_n = \frac{1}{2} \Delta_{(k_n, -k_n)} + \frac{1}{2} \Delta_{(-k_n, k_n)}$. QED.

Proof of Corollary 1. For the breakdown value we start from $F = F_1$, that is $\rho = 1$ and $X = Y$, so $\text{Cov}_F(\psi(X), \psi(Y)) = \text{Var}_F(\psi(X))$ hence $T_\psi(F) = 1$. From Proposition 2 we know that

$$\inf_{G \in \mathcal{F}_\varepsilon} T_\psi(G) = \frac{(1 - \varepsilon) \text{Var}_F(\psi(X)) T_\psi(F) - \varepsilon M^2}{(1 - \varepsilon) \text{Var}_F(\psi(X)) + \varepsilon M^2} .$$

For this to be nonpositive the numerator has to be, i.e. $(1 - \varepsilon) \text{Var}_F(\psi(X)) - \varepsilon M^2 \leq 0$. The smallest ε for which this holds is indeed $\text{Var}_F(\psi(X)) / (\text{Var}_F(\psi(X)) + M^2)$. QED.

Note that we can rewrite the breakdown value as $\varepsilon^* = 1 - (E_F[(\psi/M)^2] + 1)^{-1}$ so it is a strictly increasing function of $E_F[(\psi/M)^2]$. This implies that the maximizer of the breakdown value is $\psi(x) = \text{sign}(x)$ which maximizes $E_F[(\psi/M)^2] = 1$, hence $\varepsilon^* = 0.5$ (this yields the quadrant correlation). Interestingly, the breakdown value of the scale M-estimator S defined by $\text{ave}_i \rho(x_i/S) = E_F[\rho]$ where $\rho(z) := \psi^2(z)$ is also determined by the ratio $E_F[\rho]/M^2 = E_F[(\psi/M)^2]$, see e.g. (Maronna et al., 2006).

A.6 Relation with breakdown values of rank correlations

The breakdown values of the rank correlations in Table 1 were derived by Capéraà and Garralda (1997) and Boudt et al. (2012), but not for the ε -contamination model (20).

Instead they used *replacement contamination*, which means you can take out a certain fraction of the observations and replace them by arbitrary points. In fact ε -contamination is a special case of this, which corresponds to replacing a mass ε distributed exactly like the original distribution F , whereas in general one could replace an arbitrary part of F . Therefore the breakdown value for replacement is always less than or equal to that for ε -contamination. However, in many situations the result turns out to be the same, as is the case here.

For rank correlations in the replacement model, Capéraà and Garralda (1997) and Boudt et al. (2012) showed that given a sorted sample $(x_1, y_1), \dots, (x_n, y_n)$ where $x_1 < \dots < x_n$ and $x_i = y_i$ for all $i \in \{1, \dots, n\}$, the worst possible bias is reached by replacing the highest and the lowest y_i by values beyond the other end of the range.

We can in fact obtain the same type of configuration through the ε -contamination model. Let us start from perfectly correlated data, that is $x_i = y_i$ for all $i \in \{1, \dots, n\}$. Then choose a sequence of contaminating distributions $H_n = \frac{1}{2}\Delta_{(-k_n, k_n)} + \frac{1}{2}\Delta_{(k_n, -k_n)}$ in which the k_n are positive and tend to infinity, so the horizontal and vertical coordinates of the outliers move outside the range of the original data values. The resulting rank pairs then have the same configuration as was constructed for breakdown under replacement. Therefore the ε -contamination breakdown values of rank correlations equal those under replacement.

A.7 Simulation with cellwise outliers

This section repeats the simulation in Section 3 for cellwise outliers. The clean data are exactly the same, but now we randomly select data cells and replace them by outliers following the distribution $N(k, 0.01^2)$ when they occur in the x -coordinate and $N(-k, 0.01^2)$ when they occur in the y -coordinate. The simulation was run for 10%, 20% and 30% of cellwise outliers, but the patterns were similar across contamination levels.

Figure 10 shows the MSE of the same transformation-based correlation measures as in Figure 3, with 10% of cellwise outliers for $k = 3$ and $k = 5$. Within this class, Pearson again has the worst MSE, followed by normal scores. The quadrant correlation is next, and does not look as good here as for rowwise outliers. Wrapping has the lowest MSE,

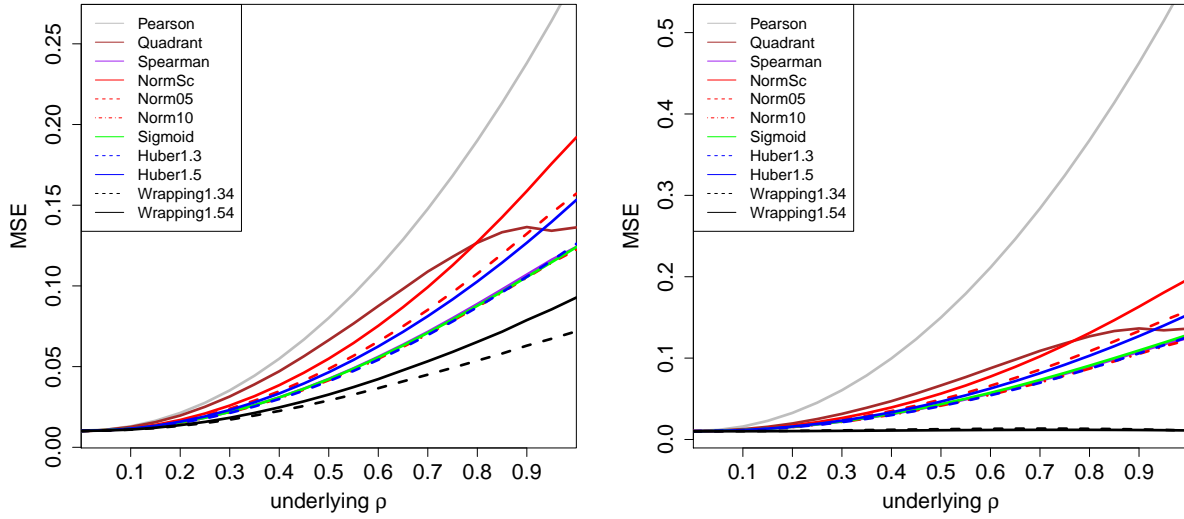


Figure 10: MSE of the correlation measures in Figure 3 with 10% of cellwise outliers placed with $k = 3$ (left) and $k = 5$ (right).

and again outperforms Spearman, sigmoid and Huber because it moves the outlying cells to the central part of their variable.

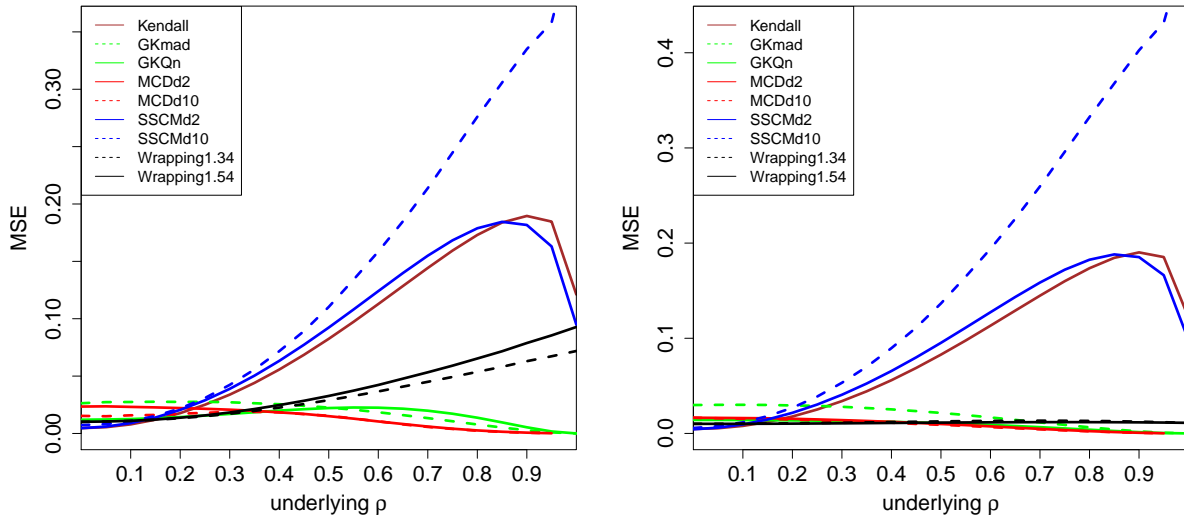


Figure 11: MSE of the correlation measures in Figure 5 with 10% of cellwise outliers placed with $k = 3$ (left) and $k = 5$ (right).

Figure 11 compares wrapping to the correlation measures in Figure 6 in the presence

of these cellwise outliers. Also here the SSCM has the largest bias, especially in $d = 10$ dimensions, followed by Kendall's tau. Wrapping does well but not as well as MCD and GK when $k = 3$, and their performance is similar for $k = 5$. But in ultrahigh dimensions wrapping still has the redeeming feature that it yields a PSD correlation matrix which the GK methods and the pairwise MCD do not, whereas running the MCD in all d dimensions becomes infeasible.